5848 *Inorg. Chem.* **2009**, *48*, 5848–5860
DOI: 10.1021/ic9001863

Inorganic Chemistry
Article

The Crucial Role of Polyatomic Anions in Molecular Architecture: Structural And Magnetic Versatility of Five Nickel(II) Complexes Derived from A N,N,O-Donor Schiff Base Ligand

Pampa Mukherjee,[†] Michael G. B. Drew,[‡] Carlos J. Gómez-García,*[,§] and Ashutosh Ghosh*[,†]

[†]*Department of Chemistry, University College of Science, University of Calcutta, 92 APC Road, Kolkata-700 009, India,* [‡]*School of Chemistry, The University of Reading, P.O BOX 224, Whiteknights, Reading RG 66AD, United Kingdom, and* [§]*Instituto de Ciencia Molecular (ICMol), Parque Científico, Universidad de Valencia, 46980 Paterna, Valencia, Spain*

Received January 29, 2009

Five new nickel(II) complexes $[Ni_2L_2(N_3)_2(H_2O)_2]$ (**1**), $[Ni_2L_2(NO_3)_2]$ (**2**), $[Ni_2L_2(O_2CPh)(CH_3OH)_2]ClO_4.0.5CH_3OH$ (**3**), $[Ni_3L_2(O_2CPh)_4]$ (**4**), and $[Ni_2L_2(NO_2)_2]_n$ (**5**) have been synthesized by using a tridentate Schiff base ligand, HL (2-[(3-Methylamino-propylimino)-methyl]-phenol), and the polyatomic monoanions N_3^-, NO_3^-, $PhCOO^-$, or NO_2^-. The complexes have been structurally and magnetically characterized. The structural analysis reveals that in all five complexes, the Ni(II) ions possess a distorted octahedral geometry. Complexes **1** and **2** are dinuclear with di-μ-1, 1-azido and di-μ_2-phenoxo bridges, respectively. Complex **3** is also a di-μ_2-phenoxo-bridged dinuclear Ni(II) complex but has an additional *syn*−*syn* benzoate bridge. Compound **4** possesses a linear trinuclear structure with the tridentate Schiff base ligand coordinated to the terminal nickel atoms which are linked to the central Ni(II) by phenoxo and carboxylate bridges. Complex **5** consists of a dinuclear entity, bridged by di-μ_2-phenoxo together with a *cis*-(μ-nitrito-1κO:2κN) nitrite ion. The dinuclear units are linked each other by another bridging trans-(μ-nitrito-1κO:2κN) nitrite to form a Ni(II) chain that shows the presence of unprecedented alternating *cis*- and *trans*-*N,O* bridging mode of the nitrite anion. Variable-temperature magnetic susceptibility measurements of complex **1** indicate the presence of ferromagnetic exchange interactions within the dimer ($J = 23.5(3)$ cm^{-1}) together with antiferromagnetic interdimer interactions ($J' = -0.513(3)$ cm^{-1}), whereas compounds **2** and **3** show intradimer antiferromagnetic interactions ($J = -24.27(6)$ and $-16.48(4)$ cm^{-1}, respectively). Ferromagnetic coupling ($J = 6.14(2)$ cm^{-1}) is observed in complex **4** for the linear centro-symmetric Ni(II) trimer, whereas complex **5** shows an alternating intra-chain antiferromagnetic coupling ($J_1 = -32.1(1)$ cm^{-1} and $J_2 = -3.2(1)$ cm^{-1}).

Introduction

In recent years, the synthesis of polynuclear complexes with a variety of bridging ligands has become an active area of research mainly because of their relevance in biological systems (as evidenced by the many existing biochemical polynuclear active complexes)[1] and because of increasing interest in the search for molecule-based and single molecule magnets.[2] The magnetic properties, associated with a large number of interacting paramagnetic centers, have significantly stimulated research efforts with the prospect of technological applications.[3] It has been verified that microscopic understanding of the magnetostructural correlations depends crucially on the superexchange coupling (J) between the spins of unpaired electrons located at metal atoms and connected through the bridging ligands (L) or interacting units.[3,4] A large amount of literature is available to show the dependence of magnitude and sign of J on the M−L−M angle and M−L bond lengths.[5] The coupling in this kind of system may be modulated in two ways: by changing the environment of the metal ion by modification of the geometry of the co-ordination polyhedra, or by modifying the bonding parameters related to the bridging ligand. Hence the selection of both metal atoms and bridging ligands is crucial for the formation of the desired polynuclear complexes with specific bridging modes of the ligands that show significant magnetic interactions. Despite interest in the properties of such systems, synthetic strategies

*To whom correspondence should be addressed. E-mail: carlos.gomez@uv.es (C.G.); ghosh_59@yahoo.com (A.G.).

(1) Messerschmidt, A.; Huber, R.; Poulos, T.; Wieghardt, K., Eds. *Handbook of Metalloproteins*; John Wiley & Sons: Chichester, U.K., 2001.
(2) (a) Kahn, O. *Molecular Magnetism*; VCH: New York, 1993; (b) D. Gatteschi, R. Sessoli and J. Villain, Molecular Nanomagnets; Oxford University Press, Oxford, UK, 2006.
(3) Ruiz, E.; Alvarez, S. *Chem. Phys. Chem.* **2005**, *6*, 1094.
(4) Rodriguez, J. H.; McCusker, J. K. *J. Chem. Phys.* **2002**, *116*, 6253.
(5) Hay, P. J.; Thibeault, J. C.; Hoffmann, R. *J. Am. Chem. Soc.* **1975**, *97*, 4884.

Published on Web 05/21/2009

Scheme 1

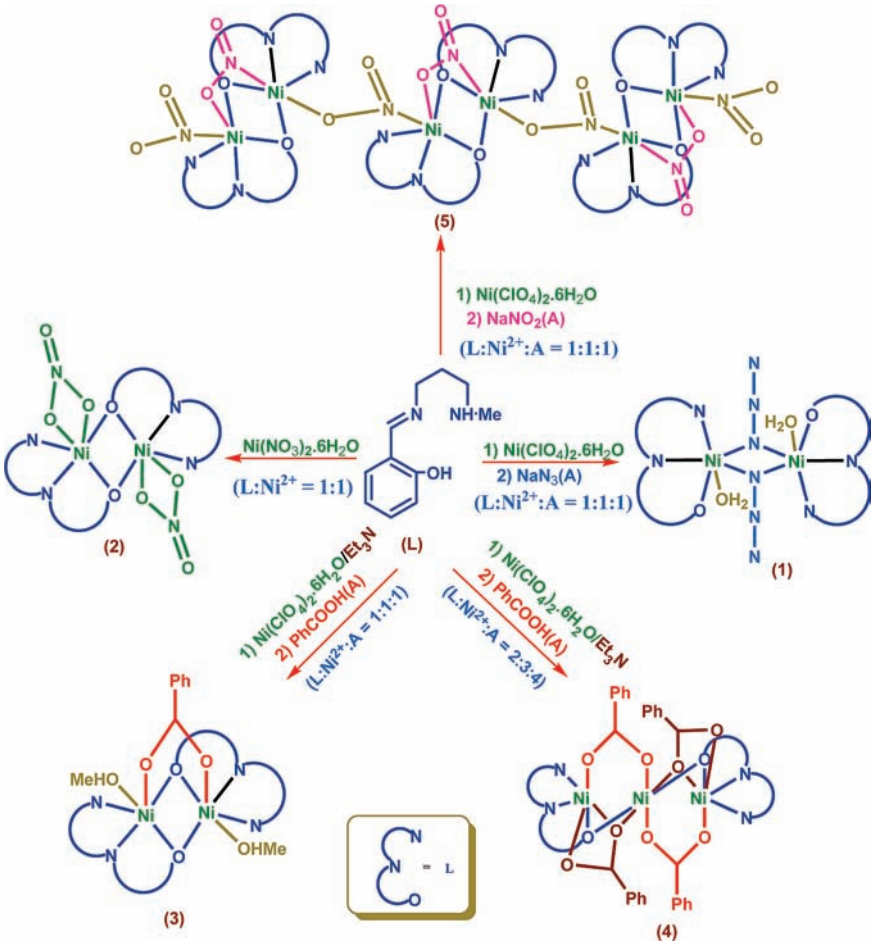

and prediction of the final structure have yet to reach the level of efficiency attained with mononuclear complexes.

Among the several paramagnetic transition metal centers, the exploration of structure and magnetic properties of octahedrally coordinated polynuclear Ni(II) complexes of monoanionic salicylaldehyde derived tridentate Schiff base ligands and polyatomic anions still remain relatively limited.[6] The tridentate ligand along with a counteranion balance the charge but the metal ion remains coordinately unsaturated unless the crystal field stabilization energy of the ligands is high enough to stabilize the square planar geometry of the Ni(II) ion. Such a situation is extremely favorable for exploiting the bridging properties of the phenoxo oxygen, the anion, or both. However, it is very difficult to predict the structure of the self-assembled species when both the phenoxo oxygen and the anion can act as bridges. Parameters that should be considered to achieve the desired species in such cases include different coordination modes of the anion, the steric and electronic requirements of the blocking Schiff base ligand, the nature of the metal ions, and their preferred coordination stereochemistry. Among these factors, a systematic study on the effect of anions on the molecular structure is scanty. To make an illuminating investigation on this effect, it is necessary to synthesize a series of compounds with variety of anions, keeping the other parameters (e.g., the Schiff base and the metal ion) constant. From this perspective, we have synthesized a new family of polynuclear Ni(II) complexes of the tridentate Schiff-base ligand, HL (2-[(3-methylamino-propylimino)-methyl]-phenol) (Scheme 1) containing the bridging polyatomic anions, N_3^-, NO_3^-, $PhCOO^-$, or NO_2^-.

Herein, we report the crystal structures and magnetic properties of a series of five new Ni(II) compounds. The series is unique in the sense that they nicely demonstrate the versatility in the structure and magnetic properties of polynuclear complexes entailed by the counteranions. For examples, among the reported complexes $[Ni_2L_2(N_3)_2(H_2O)_2]$ (**1**), $[Ni_2L_2(NO_3)_2]$ (**2**), and $[Ni_2L_2(O_2CPh)(CH_3OH)_2]ClO_4 \cdot 0.5CH_3OH$ (**3**) are dinuclear complexes having different types of bridges, whereas $[Ni_3L_2(O_2CPh)_4]$ (**4**) is a trinuclear complex and $[Ni_2L_2(NO_2)_2]_n$ (**5**) is a one-dimensional chain. The results show that a competition or cooperation between the bridging abilities of the phenoxo group and of the anions along with their diverse bridging modes determines the nuclearity and the structure of the final products. Of particular interest is the formation of dinuclear and trinuclear compounds (**3** and **4**) achieved with the same reactants by changing only the metal:ligand ratios. These two compounds illustrate the importance of the different coordination modes of the benzoate ion in determining the nuclearity of the complexes and the sign and magnitude of the magnetic coupling. Compound **5** is, as far as we know, the first case where both *cis*-*N*,*O* and *trans*-*N*,*O* bridging modes of nitrite are present in one

(6) Dey, S. K.; Mondal, N.; El Fallah, M. S.; Vicente, R.; Escuer, A.; Solans, X.; Font-Bardia, M.; Matsushita, T.; Gramlich, V.; Mitra, S. *Inorg. Chem.* **2004**, *43*, 2427 and reference therein.

compound. From the literature it is apparent that for Ni(II) complexes the *cis-N,O* bridging mode of nitrite is rare, whereas the *trans-N,O* bridge is quite common and is efficient in forming one-dimensional chain structures.[7a−7e]

Experimental Section

Materials. The reagents and solvents used were of commercially available reagent quality, unless otherwise stated.

Synthesis of the Schiff-Base Ligand 2-[(3-Methylamino-propylimino)-methyl]-phenol (HL). The Schiff base was prepared by the condensation of salicylaldehyde (1.05 mL, 10 mmol) and N-methyl-1,3-propanediamine (1.04 mL, 10 mmol) in methanol (10 mL) as reported earlier.[8,14a]

Synthesis of $[Ni_2L_2(N_3)_2(H_2O)_2]$ (1). $Ni(ClO_4)_2 \cdot 6H_2O$ (1.828 g, 5 mmol), dissolved in 10 mL of methanol, was added to a methanolic solution (10 mL) of the ligand (HL) (5 mmol) with constant stirring. After ca. 15 min, a methanol−water solution (9:1, v/v) of NaN_3 (0.32 g, 5 mmol) was added to it. Slow evaporation of the resulting green solution gave a dark blue microcrystalline compound. The solid was then filtered and washed with diethyl ether and dissolved in CH_3CN. X-ray quality plate like deep-blue single crystals of compound **1** were obtained by slow evaporation of the acetonitrile solution. (Yield: 1.24 g; 80%). Anal. Calcd. for $C_{11}H_{17}N_5NiO_2$: C, 42.62 ; H, 5.53 ; N, 22.59 . Found: C, 42.58; H, 5.69 ; N, 22.45. IR (KBr pellet, cm^{-1}): 3488 (broad) ν(OH), 3231 ν(NH), 1629 ν(C═N), and 2057 $\nu_{as}(N_3^-)$. λ_{max} (solid, reflectance), 610 and 1115 nm.

Synthesis of $[Ni_2L_2(NO_3)_2]$ (2). $Ni(NO_3)_2 \cdot 6H_2O$ (1.455 g, 5 mmol), dissolved in 10 mL of methanol, was added to a methanolic solution (10 mL) of the ligand (HL) (5 mmol). The color of the solution turned to deep blue. The solution was left to stand in air until plate-shaped petrol-blue X-ray quality single crystals of complex **2** appeared at the bottom of the vessel on slow evaporation of the solvent. (Yield: 1.32 g; 85%) Anal. Calcd. for $C_{11}H_{15}N_3NiO_4$: C, 42.35; H, 4.85; N, 13.47. Found: C, 42.22 ; H, 4.79 ; N, 13.55. IR (KBr pellet, cm^{-1}): 3284 ν(NH), 1643 ν(C═N), 1291 $\nu(NO_3^-)$, λ_{max} (solid, reflectance), 603, 1008 nm.

Synthesis of $[Ni_2L_2(O_2CPh)(CH_3OH)_2]ClO_4 \cdot 0.5CH_3OH$ (3). The procedure was the same as that for complex **1**, except that a methanolic solution of benzoic acid, PhCOOH (0.610 g, 5 mmol) was added instead of sodium azide with slow stirring followed by triethylamine (0.7 mL, 5 mmol). Needle-shaped deep-green X-ray quality single crystals were obtained after several days. Crystals were filtered out and air-dried. (Yield: 1.53 g; 75%) Anal. Calcd. for $C_{32}H_{47}ClN_4Ni_2O_{11}$: C, 47.07 ; H, 5.80 ; N, 6.86 . Found: C, 47.12 ; H, 5.89 ; N, 6.45 . IR (KBr pellet, cm^{-1}): 3403 (broad) ν(OH), 3274 ν(NH), 1638 ν(C═N), 1560 ν_{as}(C═O), 1466 ν_s(C═O), 1089 $\nu(ClO_4^-)$. λ_{max} (solid, reflectance), 618 and 959 nm.

Synthesis of $[Ni_3L_2(O_2CPh)_4]$ (4). The procedure was the same as that for complex **3**, except the proportion of the added reagents. A methanolic solution of $Ni(ClO_4)_2 \cdot 6H_2O$ (2.742 g, 7.5 mmol) was added to a methanolic solution (10 mL) of the ligand HL (5 mmol) with constant stirring. A 10 mL methanolic solution of benzoic acid, PhCOOH (1.220 g, 10 mmol) was added to the solution followed by triethylamine (1.4 mL, 10 mmol). A deep green precipitate appeared immediately. It was then filtered and washed with diethyl ether and then redissolved in CH_3CN. Needle-shaped deep-green single crystals of **4**, suitable for X-ray diffraction were obtained by layering of the green solution with Et_2O. (Yield: 1.96 g; 75%) Anal. Calcd for $C_{50}H_{50}N_4Ni_3O_{10}$: C, 57.58; H, 4.83; N, 5.37. Found: C, 57.12; H, 4.89; N, 5.45. IR (KBr pellet, cm^{-1}): 3280 ν(NH), 1632 ν(C═N), 1559 ν_{as}(C═O), 1480 ν_s(C═O). λ_{max} (solid, reflectance), 610 and 964 nm.

Synthesis of $[Ni_2L_2(NO_2)_2]_n$ (5). The procedure was the same as that for complex **1** except that a methanol-water solution (9:1, v/v) of $NaNO_2$ (0.345 g, 5 mmol) was added instead of sodium azide with slow stirring. The solution was left to stand overnight in air, when block shaped deep blue X-ray quality single crystals of complex **5** appeared at the bottom of the vessel. (Yield: 1.03 g; 70%) Anal. Calcd. for $C_{22}H_{30}N_6Ni_2O_6$: C, 44.64 ; H, 5.11; N, 14.20. Found: C, 44.58; H, 5.09; N, 14.45. IR (KBr pellet, cm^{-1}): 3341 ν(NH), 1630 ν(C═N), 1316 $\nu_s(NO_2)$, 1151 $\nu_{as}(NO_2)$, λ_{max} (solid, reflectance), 608, 985 nm.

Physical Measurements. Elemental analyses (C, H and N) were performed using a Perkin-Elmer 240C elemental analyzer. IR spectra in KBr pellets (4500−500 cm^{-1}) were recorded using a Perkin-Elmer RXI FT- IR spectrophotometer. Electronic spectra in solid state (1500−250 nm) were recorded in a Hitachi U-3501 spectrophotometer. Variable-temperature susceptibility measurements were carried out with an applied magnetic field of 0.1 T in the temperature range 2−300 K on polycrystalline samples of the five compounds (with masses of 42.86, 47.75, 68.34, 23.27, and 78.73 mg for compounds **1**−**5**, respectively) with a Quantum Design MPMS-XL-5 SQUID magnetometer (for compounds **1**, **2** and **4**) and with a Quantum Design PPMS-9 system (for compounds **3** and **5**). The isothermal magnetizations were made at 2 K with magnetic fields of up to 5 T (for compounds **1**, **2**, and **4**) and up to 9 T (for compounds **3** and **5**). The susceptibility data were corrected for the sample holder previously measured using the same conditions and for the diamagnetic contributions of the salt as deduced by using Pascal′s constant tables ($\chi_{dia} = -366.0 \times 10^{-6}$, -343.2×10^{-6}, -467.6×10^{-6}, -595.0×10^{-6}, and -332.6×10^{-6} emu mol^{-1} for compounds **1**−**5**, respectively).

Crystal Data Collection and Refinement. Crystal data for the five complexes are given in Table 1. 3840, 3714, 5099, 6650, and 6948 independent data for **1**−**5** were collected with Mo Kα radiation using an Oxford Diffraction X-Calibur CCD System. The crystals were positioned at 50 mm from the CCD. 321 frames were measured with a counting time of 10 s. Data analysis was carried out with the Crysalis program.[9] The structures were solved using direct methods with the SHELXS97 program.[10] The non-hydrogen atoms were refined with anisotropic thermal parameters. The hydrogen atoms bonded to carbon were included in geometric positions and given thermal parameters related to those of the atom to which they were attached, 1.5 times for methyl hydrogens, 1.2 times for others. Hydrogen atoms of the water molecule in **1** were located in the difference Fourier map and refined with distance constraints. One nitrite group in **5** was disordered over two possible sites (see discussion). Absorption corrections were carried out using the ABSPACK program.[11] The structures were refined on F^2 using SHELXL97[10] to R_1 values of 0.0749, 0.0465, 0.0572, 0.0676, and 0.0446 and wR_2 values of 0.1498, 0.0867, 0.1355, 0.1161, and 0.0964 for 3207, 1287, 3110, 2910, and 4477 reflections with $I > 2\sigma(I)$ for complexes **1**−**5**, respectively.

(7) (a) Llewellyn, F. J.; Waters, J. M. *J. Chem. Soc.* **1962**, 3845. (b) Finney, A. J.; Hitchman, M. A.; Raston, C. L.; Rowbottom, G. L.; White, A. H. *Aust. J. Chem.* **1981**, *34*, 2159. (c) Rajendiran, T. M.; Kahn, O.; Golhen, S.; Ouahab, L.; Honda, Z.; Katsumata, K. *Inorg. Chem.* **1998**, *37*, 5693. (d) Meyer, A.; Gleizes, A.; Girerd, J.-J.; Verdaguer, M.; Kahn, O. *Inorg. Chem.* **1982**, *21*, 1729. (e) Landee, C. P.; Reza, K. A.; Bond, M. R.; Willett, R. D. *Phys. Rev. B: Condens. Mater.* **1997**, *56*, 147. (f) Escuer, A.; Vicente, R.; Solans, X. J. *Chem. Soc., Dalton Trans.* **1997**, 531. (g) Sarkar, B.; Konar, S.; Gómez-García C. J.; Ghosh, A. *Inorg. Chem.* **2008**, *47*, 11611 and references therein.

(8) Hamalainen, R.; Ahlgren, M.; Turpeinen, U. *Acta Crystallogr., Sect. B* **1982**, *38*, 1577.

(9) *Crysalis, v1*; Oxford Diffraction Ltd.: Oxford, U.K., 2005.

(10) Sheldrick, G. M. *SHELXL-97 and SHELXS-97 Programs for Crystallographic Calculations*; University of Göttingen: Göttingen, Germany, 1997.

(11) *ABSPACK*; Oxford Diffraction Ltd.: Oxford, U.K., 2005.

Table 1. Crystal Data and Structure Refinement of Complexes **1**−**5**

	1	**2**	**3**	**4**	**5**
formula	$C_{22}H_{34}N_{10}Ni_2O_4$	$C_{22}H_{30}N_6Ni_2O_8$	$C_{32}H_{47}N_4Ni_2O_{11}Cl$	$C_{50}H_{50}N_4Ni_3O_{10}$	$C_{22}H_{30}N_6N_2O_6$
fw	619.97	623.90	816.57	1043.01	591.90
space group	$P2_1/c$	*Ccca*	$P4_12_12$	*Pbna*	$P2_1/a$
cryst syst	monoclinic	orthorhombic	tetragonal	orthorhombic	monoclinic
a (Å)	6.8549(3)	15.6192(18)	16.0978(8)	14.1337(6)	12.0663(4)
b (Å)	19.7038(9)	19.3293(12)	16.0978(8)	23.2885(10)	14.9246(4)
c (Å)	10.2237(6)	16.980(4)	13.5668(10)	14.0731(6)	13.9308(4)
α (deg)	(90)	(90)	(90)	(90)	(90)
β (deg)	97.880(4)	(90)	(90)	(90)	106.760(3)
γ (deg)	(90)	(90)	(90)	(90)	(90)
V (Å^3)	1367.85(12)	5126.4(14)	3515.7(4)	4632.2(3)	2402.16(13)
Z	2	8	4	4	4
calcd density	1.505	1.617	1.543	1.496	1.637
absorp coeff (μ) (mm^{-1})	1.424 (Mo Kα)	1.528 (Mo Kα)	1.212 (Mo Kα)	1.271 (Mo Kα)	1.619 (Mo Kα)
F(000)	648	2592	1712	2168	1232
cryst size (mm^3)	0.03 × 0.16 × 0.22	0.03 × 0.17 × 0.17	0.05 × 0.05 × 0.30	0.05 × 0.05 × 0.30	0.13 × 0.15 × 0.16
θ range (deg)	2.3, 30.0	2.6, 30.0	2.3, 30.0	2.7, 30.0	2.2, 30.0
R(int)	0.042	0.091	0.077	0.108	0.048
no. of unique data	3840	3714	5099	6650	6948
data with $I > 2\sigma(I)$	3207	1287	3111	2911	4477
R_1 on $I > 2\sigma(I)$	0.0749	0.0465	0.0572	0.0676	0.0446
wR_2 on $I > 2\sigma(I)$	0.1565	0.0984	0.1520,	0.1407	0.1084
GOF on F^2	1.204	0.714	0.802	0.932	0.951

Results and Discussion

Synthesis of the Complexes. Five new Ni(II) complexes have been prepared with the monocondensed tridentate Schiff base ligand HL (2-[(3-methylamino-propylimino)-methyl]-phenol). Complex **2** was prepared by reacting a methanol solution of nickel nitrate and the ligand (HL) in a 1:1 molar ratio. Complexes **1**, **3**, and **5** were synthesized in a very similar way, by adding a methanolic solution of $Ni(ClO_4)_2 \cdot 6H_2O$ to a methanolic solution of the Schiff base ligand HL followed by aqueous-methanolic solutions of NaN_3 (for **1**), benzoic acid (for **3**), or $NaNO_2$ (for **5**) in a 1:1:1 molar ratio. Complexes **3** and **4** were synthesized using the same reagents but in different ratios. Thus, complex **3** was prepared with a 1:1:1 Ni:HL:PhCOOH ratio, whereas complex **4** was obtained with a 1.5:1:2 Ni:HL:PhCOOH ratio. The deprotonation of the benzoic acid in both cases was achieved with the required equimolar amounts of triethylamine. Interestingly, a similar change in the Ni:L ratio for the other complexes did not lead to the formation of any complexes other than **1**, **2**, and **5** in case of azide, nitrate and nitrite respectively. This fact may be attributed to the higher coordination flexibility of the benzoate ligand compared to the azide, nitrate and nitrite ligands as demonstrated by the fact that in complex **4** the benzoate ligand shows two different types of bridging mode − one is bidentate and the other is tridentate (see structural description of complex **4**)

IR and UV−Vis Spectra of Complexes. In the IR spectra of complexes **1**−**5**, the NH stretching mode is seen at 3231, 3284, 3274, 3280, and 3241 cm^{-1}, respectively, as a sharp band. A strong and sharp band due to azomethine $\ddot{v}$(C═N) appears at 1629, 1643, 1638, 1632, and 1630 cm^{-1} for complexes **1**−**5**, respectively. In the IR spectra of complex **1**, the appearance of a broad band near 3488 cm^{-1} indicates the presence of water molecules. Complex **1** shows only a single absorption band, at 2057 cm^{-1}, coming from the azide ligand, consistent with the presence of only one type of azide bridge in the structure.[12] In complex **2**, the characteristic strong peak of the coordinated nitrate anion is observed at 1291 for assymetric stretching vibration. In the IR spectra of complex **3**, the broad band near 3400 cm^{-1} may be attributed to the presence of the O−H stretching of the methanol molecules. In complexes **3** and **4**, the bands in the IR spectra in the 1300−1650 cm^{-1} region are difficult to be attributed to the appearance of several absorption bands from both the Schiff base and the carboxylate ligands. Nevertheless, the strong bands at 1560 and 1559 cm^{-1} are likely to be due to the antisymmetric stretching mode of the carboxylate group, whereas the bands at 1466 and 1480 cm^{-1} can be attributed to the symmetric stretching modes of the carboxylate ligands in complexes **3** and **4**, respectively.[13] In complex **3**, the characteristic strong peak of the stretching vibration of uncoordinated perchlorate is observed at 1089 cm^{-1}. In complex **5**, absorption bands at 1316, 1151, and 892 cm^{-1} are tentatively assigned to νs(NO_2), νas(NO_2), and δ(NO_2), respectively.[7]

The solid-state reflectance spectra of the complexes show a broadband centered at 1115, 1008, 959, 964, and 985 nm for complexes **1**−**5**, respectively. These broad bands are well-separated from the second transition observed at ca. 610, 603, 618, 610, and 608 nm for **1**−**5**, respectively. All these bands are the typical ones in octahedral Ni(II) complexes.[14]

(12) Mukherjee, P.; Drew, M. G. B.; Ghosh, A. *Eur. J. Inorg. Chem.* **2008**, 3372 and references therein.

(13) (a) Sarkar, S.; Mondal, A.; Banerjee, A.; Chopra, D.; Ribas, J.; Rajak, K. K. *Polyhedron* **2006**, *25*, 2284. (b) Li, J. −M.; Jiang, Y. −M.; Wang, Y. −F.; Liang, D. W. *Acta Crystallogr., Sect. E* **2005**, *61*, m2160. (c) Sen, S.; Mitra, S.; Hughes, D. L.; Rosair, G.; Desplanches, C. *Polyhedron* **2007**, *26*, 1740. (d) Costes, J. P.; Dahan, F.; Laurent, J. P. *Inorg. Chem.* **1985**, *24*, 1018. (e) Sarkar, B.; Drew, M. G. B.; Estrader, M.; Diaz, C.; Ghosh, A. *Polyhedron* **2008**, *27*, 2625 and references therein.

(14) (a) Mukherjee, P.; Drew, M. G. B.; Estrader, M.; Ghosh, A. *Inorg. Chem.* **2008**, *47*, 7784. (b) Dey, M.; Rao, C. P.; Saarenketo, P. K.; Rissanen, K. *Inorg. Chem. Commun.* **2002**, *5*, 924. (c) Koizumi, S.; Nihei, M.; Oshio, H. *Chem. Lett.* **2003**, *32*, 812. (d) Banerjee, S.; Drew, M. G. B.; Lu, C.-Z.; Tercero, J.; Diaz, C.; Ghosh, A. *Eur. J. Inorg. Chem.* **2005**, 2376 and references therein.

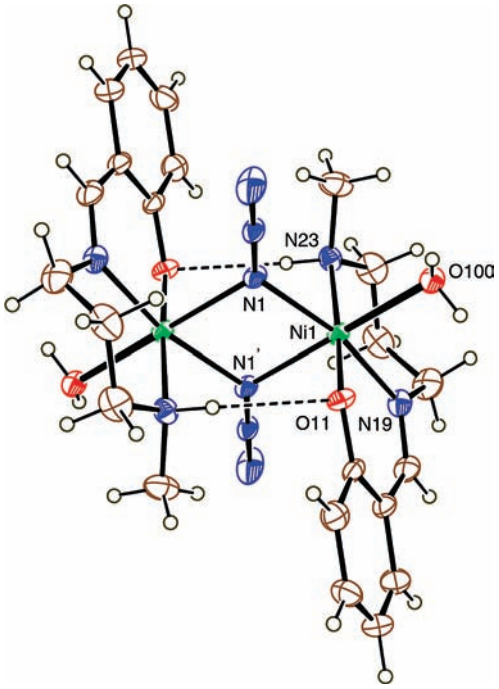

Figure 1. ORTEP-3 view of the asymmetric unit of **1** with ellipsoids at the 50% probability level.

The higher-energy d−d bands are obscured by strong charge-transfer transitions.

Structure of $[Ni_2L_2(N_3)_2(H_2O)_2]$ (1). The structure determination reveals that complex **1** consists of a neutral azido-bridged centro-symmetric dimer, $[Ni_2L_2(N_3)_2(H_2O)_2]$ as shown in Figure 1. The nickel atoms present identical distorted octahedral environments formed by a deprotonated chelate Schiff base ligand ($1\kappa^3N,N',O:2\kappa O$), a nitrogen atom, N(1), of one of the bridging azides, a nitrogen atom, N(1)′ (′ = $-x$, $1-y$, $-z$) from the symmetry-related bridging azide ligand and by a water molecule O(100). The Schiff base ligand coordinates the Ni(II) ion in meridional (*mer*) configuration through the amine nitrogen N(23), the imine nitrogen N(19) and the phenoxo oxygen atom O(11) with bond distances (Table 2) similar to those observed in other related compounds and in the other complexes reported here.[13] As can be seen in Figure 1, each azide ion bridges the nickel atoms in an end-on (μ-1,1 or $1\kappa N:2\kappa N$) fashion. The di-μ-1,1-azido bridge in this complex leads to a perfectly planar Ni_2N_2 ring because the dimer sits on a crystallographic inversion center. The azide ions are nearly linear with a N(1)−N(2)−N(3) angle of 178.4(5)°. The slightly asymmetric double azide bridge (with Ni−N1 bond distances of 2.096(3) and 2.143(3) Å and a Ni−N1−Ni bond angle of 101.61(15)°) separates the two Ni(II) ions by 3.285 (4) Å, indicating the absence of any bond between them. The six-membered chelate ring comprising the nickel, imine N atom, three propylene C atoms and the amino N atoms adopt half-chair conformation, whereas the other chelate ring containing the aromatic ring is slightly distorted from planarity (maximum r.m.s. deviation 0.11 Å).

The amine hydrogen atom H(11) participates in a weak intradimer hydrogen bonding to the phenoxo oxygen O(11)′ atom (′ = $-x$, $1-y$, $-z$) within the dimeric unit with an H···O distance of 2.350 Å (Figure 1). Both hydrogen atoms of the water molecule O(100) are involved in strong intermolecular hydrogen bonding (see Table S1 in the Supporting Information). One of them, H(1) forms a bifurcated H-bond with the N(2)″ and N(3)″ atoms (″ = $1-x$, $1-y$, $1-z$) of the azide ligand of the neighboring unit (with H···N distances of 2.44(4) and 2.36(4) Å, respectively). The other hydrogen atom, H (2), forms another hydrogen bond with the O(11)″ atom (″ = $1-x$, $1-y$, $1-z$), the phenoxo oxygen atom of the Schiff base ligand of a neighboring unit with an H···O distance of 1.84(4) Å. These two H-bonds link the Ni(II) dimers to form an infinite 1D hydrogen bonded chain as shown in Figure S1 of the Supporting Information.

Table 2. Bond Distances (Å) and Angles deg) in the Metal Coordination Spheres of Complex **1**[a]

atoms	distance	atoms	angle
Ni(1)−N(1)	2.096(3)	N(19)−Ni(1)−N(1)	167.73(14)
Ni(1)−N(1)′	2.143(3)	O(11)−Ni(1)−N(1)	86.08(13)
Ni(1)−N(23)	2.105(4)	N(19)−Ni(1)−N(23)	97.06(15)
Ni(1)−N(19)	2.028(3)	O(11)−Ni(1)−N(23)	171.54(13)
Ni(1)−O(11)	2.029(3)	N(1)−Ni(1)−N(23)	86.50(14)
Ni(1)−O(1)	2.126(3)	N(19)−Ni(1)−O(1)	90.32(13)
		O(11)−Ni(1)−O(1)	88.01(12)
		N(1)−Ni(1)−O(1)	101.49(12)
		N(23)−Ni(1)−O(1)	89.49(13)
		N(19)−Ni(1)−N(1)′	89.82(13)
		O(11)−Ni(1)−N(1)′	92.12(13)
		N(1)−Ni(1)−N(1)′	78.39(13)
		N(23)−Ni(1)−N(1)′	90.36(14)
		O(1)−Ni(1)−N(1)′	179.81(15)

[a] Symmetry code ′ = $-x$, $1-y$, $-z$.

Among the several reports on di-μ-1,1-N_3 bridged dinuclear Ni(II) compounds with tridentate ligands, the majority contain N,N,N donor ligands.[6,15] Azide-bridged dinuclear Ni(II) compounds with N,N,O donor ligands are relatively scarce.[15] It is to be noted that in the case of N,N,O donor salicylaldehyde-derived Schiff base ligands, there is a competition between the phenoxo oxygen atom and the azide ligand to act as a bridge. The literature data show that except in one case,[17] the azide ligand dominates over the phenoxo group in bridging the metal centers.

Structure of $[NiL_2(NO_3)_2]$ (2). The crystal structure of **2** consists of a discrete centro-symmetric dimeric unit of

(15) (a) Barandika, M. G.; Cortes, R.; Lezama, L.; Urtiaga, M. K.; Arriortua, M. I.; Rojo, T. *J. Chem. Soc., Dalton Trans.* **1999**, 2971. (b) Bian, H.-D.; Gu, W.; Yu, Q.; Yan, S.-P.; Liao, D.-Z.; Jiang, Z.-H.; Cheng, P. *Polyhedron* **2005**, *24*, 2002. (c) Arriortua, M. I.; Cortes, A. R.; Lezam, L.; Rojo, T.; Solans, X.; -Bardia, M. F. *Inorg. Chim. Acta* **1990**, *174*, 263. (d) Kurtaran, R.; Arici, C.; Emregul, K. C.; Ulku, D.; Atakol, O.; Tastekin, M. *Z. Anorg. Allg. Chem.* **2003**, *629*, 1617. (e) Wang, Q.-L.; Yu, L.-H.; Liao, D.-Z.; Yan, S.-P.; Jiang, Z.-H.; Cheng, P. *Helv. Chim. Acta* **2003**, *86*, 2441. (f) Cortes, R.; Larramendi, J.; Lezama, L.; Rojo, T.; Urtiaga, K.; Arriortua, M. I. *J. Chem. Soc., Dalton Trans.* **1992**, 2723. (g) Vicente, R.; Escuer, A.; Ribas, J.; Fallah, M. S.; Solans, X.; Bardia, M. F. *Inorg. Chem.* **1993**, *32*, 1920. (h) Chaudhuri, P.; Weyhermuller, T.; Bill, E.; Wieghardt, K. *Inorg. Chim. Acta* **1996**, *252*, 195. (i) Escuer, A.; Vicente, R.; Ribas, J.; Solans, X. *Inorg. Chem.* **1995**, *34*, 1793.

(16) (a) Garnovskii, A. D.; Burlov, A. S.; Garnovskii, D. A.; Vasilchenko, I. S.; Antsichkina, A. S.; Sadikov, G. G.; Sousa, A.; Garcia-Vazquez, J. A.; Romero, J.; Duran, M. L.; Sousa-Pedrares, A.; Gomez, C. *Polyhedron* **1999**, *18*, 863. (b) Lozan, V.; Lassahn, P.-G; Zhang, C.; Wu, B.; Janiak, C.; Rheinwald, G.; Lang, H. *Z.Naturforsch.,B:Chem.Sci.* **2003**, *58*, 1152. (c) Tai, X. -S.; Wang, L.-H.; Li, Y.-Z.; Tan, M.-Y. *Z. Kristallogr.−New Cryst. Struct.* **2004**, *219*, 445. (d) Floyd, J. M.; Gray, G. M.; Spivey, A. G. V.; Lawson, C. M.; Pritchett, T. M.; Ferry, M. J.; Hoffman, R. C.; Mott, A. G. *Inorg. Chim. Acta* **2005**, *358*, 3773.

(17) Bu, X.; Du, H.; Zhang, M. L.; Liao, D.-Z.; Tang, J.-K.; Zhang, R.-H.; Shionoya, M. *J. Chem. Soc., Dalton Trans.* **2001**, 593.

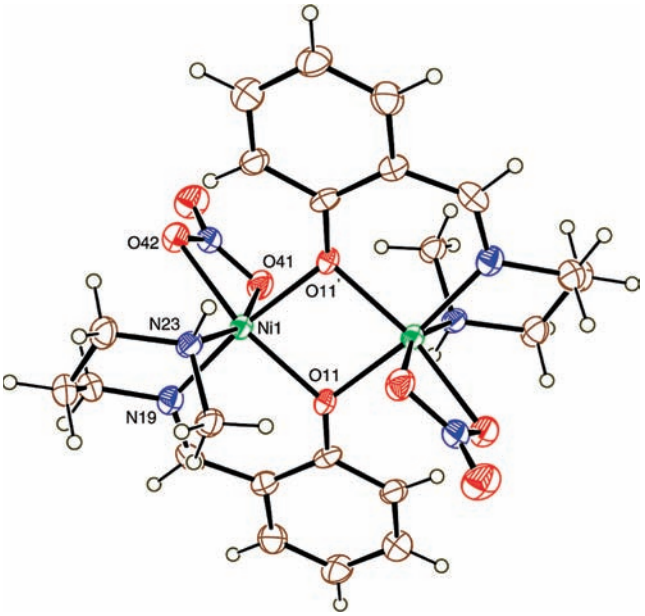

Figure 2. ORTEP-3 view of the asymmetric unit of **2** with ellipsoids at the 50% probability level.

formula $[Ni_2L_2(NO_3)_2]$ (Figure 2). Selected bond lengths and angles are summarized in Table 3. The dinuclear unit is formed by two Ni(II) atoms labeled Ni(1) and Ni(1′) (′ = $1-x, 1-y, -z$), bridged by the two phenoxo oxygen atoms O(11) and O(11′) of the Schiff-base ligands, L. Each of the two equivalent nickel atoms presents a distorted octahedral environment formed by the deprotonated chelate Schiff base ligand ($1\kappa^3N,N',O$:2κO), a bidentate nitrate anion (κ^2O,O') and a phenoxo oxygen atom from the symmetry related Schiff base ligand (1κO:$2\kappa^3N,N',O$) (Figure 2). The Schiff base ligand coordinates the Ni(II) ion in facial (*fac*) configuration through the amine nitrogen N(23), the imine nitrogen N(19), and the phenoxo oxygen atom O(11) with usual bond distances (Table 3) phenoxo-bridged.[14] Note that the double oxo bridge connecting both Ni(II) ions is slightly asymmetric because each Ni(II) ion is closer to its own phenoxo oxygen atom (Ni(1)−O(11) = 2.009(2) Å) than to the phenoxo oxygen atom of the symmetry-related Schiff base (Ni(1)−O(11) = 2.070(3) Å). The two Ni atoms are separated by 3.119(1) Å and the Ni−O(11)−Ni′ angle is 99.75(10)°. The six-member ring comprising the nickel, the imine N atom, three propylene C atoms, and the amino N atom adopts a chair conformation, whereas that containing the aromatic moiety is slightly deviated from planarity (maximum r.m.s. deviation 0.13 Å) toward a boat conformation. In **2**, the amino hydrogen does not form any hydrogen bonds.

There are a few Schiff base complexes of Ni(II) together with nitrate as coligand. Interestingly, in most of them, the Schiff base is tetradentate and the nitrate ion acts as an additional bridge between two Ni(II) centers. Only in two cases has the chelating nitrate been found, but bidentate Schiff bases were used in both cases. No Ni(II) complex containing a salicylaldehyde-derived tridentate Schiff base along with nitrate as coligand has been reported until now. Another unusual feature of this complex is the *fac* coordination of the Schiff base ligand since in most of the known double phenoxo-bridged Ni(II) dimers with tridentate ligands, a meridional coordination is found.[14b−14d,16] The chelating coordination of the nitrate coligand that must span *cis*-positions is likely to be responsible for this unusual facial coordination of the Schiff base ligand with a folded conformation.

Table 3. Bond Distances (Å) and Angles (deg) in the Metal Coordination Spheres of Complex **2**[a]

atoms	distance	atoms	angle
Ni(1)−O(11)	2.009(2)	N(19)−Ni(1)−O(11)	91.96(11)
Ni(1)−O(42)	2.150(2)	N(19)−Ni(1)−N(23)	87.63(12)
Ni(1)−N(23)	2.067(3)	O(11)−Ni(1)−N(23)	102.98(10)
Ni(1)−N(19)	1.993(3)	N(19)−Ni(1)−O(11)′	172.15(10)
Ni(1)−O(11)′	2.070(3)	O(11)−Ni(1)−O(11)′	80.25(10)
Ni(1)−O(41)	2.183(2)	N(23)−Ni(1)−O(11)′	93.17(11)
		N(19−Ni(1)−O(42)	91.06(10)
		O(11)−Ni(1)−O(42)	156.43(9)
		N(23)−Ni(1)−O(42)	100.49(10)
		O(11)′−Ni(1)−O(42)	96.47(9)
		N(19)−Ni(1)−O(41)	90.04(11)
		O(11)−Ni(1)−O(41)	96.85(9)
		N(23)−Ni(1)−O(41)	160.09(9)
		O(11)′−Ni(1)−O(41)	91.82(9)
		O(42)−Ni(1)−O(41)	59.77(9)

[a] Symmetry code ′ = $1-x, 1-y, -z$.

Table 4. Bond Distances (Å) and Angles (deg) in the Metal Coordination Spheres of Complex **3**[a]

atoms	distance	atoms	angle
Ni(1)−O(41)	2.032(3)	O(41)−Ni(1)−O(11)	93.51(13)
Ni(1)−O(11)	2.049(3)	O(41)−Ni(1)−N(19)	90.07(14)
Ni(1)−N(19)	2.064(4)	O(11)−Ni(1)−N(19)	88.33(15)
Ni(1)−O(11)′	2.114(3)	O(41)−Ni(1)−O(11)′	92.32(12)
Ni(1)−N(23)	2.123(4)	O(11)−Ni(1)−O(11)′	78.05(14)
Ni(1)−O(31)	2.133(3)	N(19)−Ni(1)−O(11)′	166.29(15)
		O(41)−Ni(1)−N(23)	87.12(15)
		O(11)−Ni(1)− N(23)	175.37(13)
		N(19)−Ni(1)−N(23)	96.26(16)
		N(23)−Ni(1) −O(11)′	97.34(14)
		O(41)−Ni(1)−O(31)	177.74(15)
		O(11)−Ni(1)−O(31)	88.37(14)
		N(19)−Ni(1)−O(31)	88.72(14)
		O(31)−Ni(1)−O(11)′	89.31(12)
		N(23)−Ni(1)−O(31)	91.11(15)

[a] Symmetry code ′ = $y, x, -z$.

Structure of $[Ni_2L_2(O_2CPh)(CH_3OH)_2]ClO_4\cdot 0.5CH_3OH$ (3). The crystal structure of **3** consists of a discrete dinuclear cationic unit containing a C_2 axis formulated as $[Ni_2L_2(O_2CPh)(CH_3OH)_2]^+$ together with a solvent molecule of CH_3OH with 50% occupancy. The charge on the cation is counterbalanced by a ClO_4^- anion (Figure 3). Selected bond lengths and angles are summarized in Table 4. The dinuclear unit is formed by two Ni(II) atoms labeled Ni(1) and Ni(1′) (′ = $y, x, -z$), bridged by two μ_2-phenoxo oxygen atoms O(11) and O(11′) of the Schiff-base ligands and by two oxygen atoms O(41) of a bridging bidentate benzoate ligand ($1\kappa O$:$2\kappa O'$). The two equivalent nickel atoms present a distorted octahedral environment formed by the amino nitrogen atoms N(23) and imino nitrogen atoms N(19) and a phenoxo oxygen atom O(11) of the deprotonated chelated tridentate Schiff base ligand (L) in *mer* configuration, the phenoxo oxygen atom, O(11)′, from the symmetry-related Schiff base ligand, an oxygen atom O(41) from a bridging bidentate benzoate ligand, and an oxygen atom O(31) from a methanol ligand

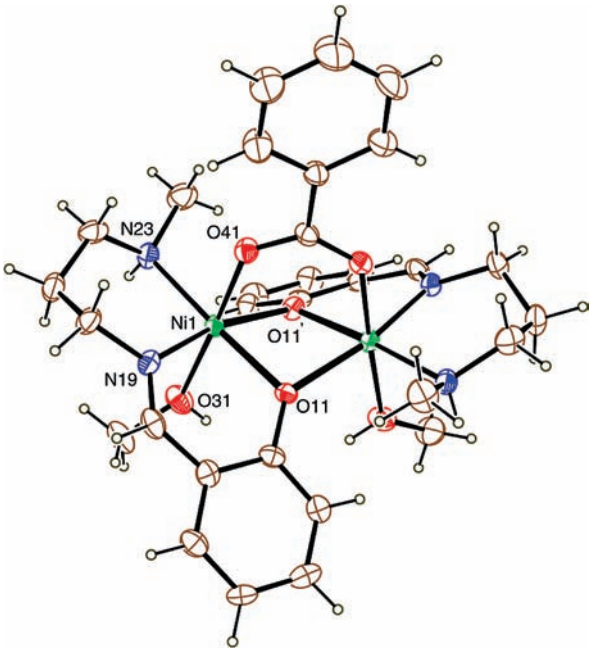

Figure 3. ORTEP-3 view of the asymmetric unit of **3** with ellipsoids at the 50% probability level.

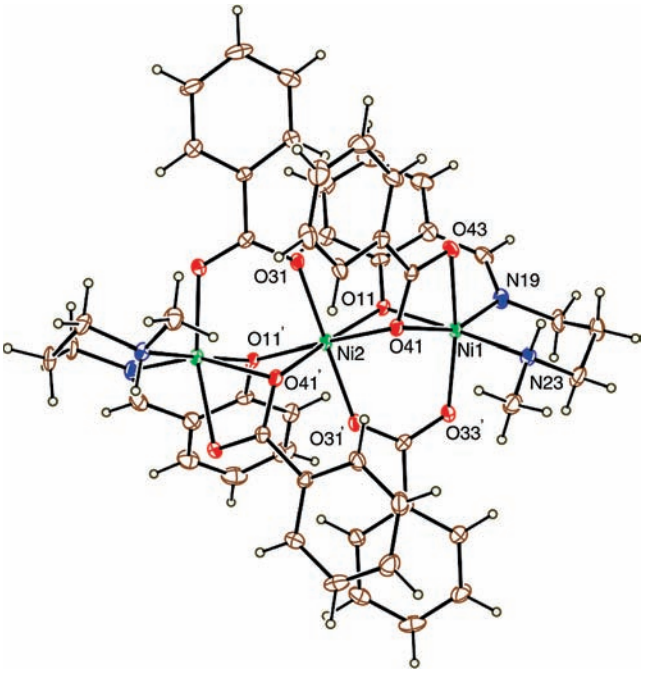

Figure 4. ORTEP-3 view of the asymmetric unit of **4** with ellipsoids at the 50% probability level.

(trans to the benzoate O(41) atom, Figure 3). The Ni−O (11), Ni−N(19), and Ni−N(23) bond distances (Table 4) are similar to those found in other related complexes and in the other complexes reported here.[14b−d,16,17] As in complex **2**, the double phenoxo bridge connecting both Ni(II) ions is slightly asymmetric with each Ni(II) ion being closer to its own phenoxo oxygen atom (Ni(1)−O (11) = 2.049(3) Å) than to the phenoxo oxygen atom of the symmetry-related Schiff base (Ni(1)−O(11′) = 2.114(3) Å). The two Ni atoms are separated by 3.109(1) Å and the Ni−O(11)−Ni′ angle is 96.60(12)°. The six-member ring comprising the Ni(II) ion, the imine N atom, three propylene C atoms, and the amino N atom adopts a half-chair conformation whereas that containing the aromatic moiety is distorted from planarity (maximum r.m.s. deviation 0.17 Å) toward a boat conformation. The amine N(23)-H forms a hydrogen bond to a perchlorate oxygen O(72) with dimensions N···O = 3.085(6)Å, H···O = 2.23 Å and N−H···O = 157°, whereas the methanol oxygen O(31)−H forms a hydrogen bond to the solvent methanol oxygen atom O(100) with dimensions 2.919(8), 2.13 Å, and 149°.

There are several reports[14b−d,16,17] of double phenoxo-bridged Ni(II) dimers but the presence of an additional *syn*−*syn* carboxylate bridge in dinuclear Ni(II) complexes is very rare. Only two such complexes are reported: one with trichloroacetate[18a] and other with an acetate ion.[18b] On the contrary, this type of triple bridge is very usual in trinuclear Ni(II) complexes.[19]

Structure of $[Ni_3L_2(O_2CPh)_4]$ (4). The molecular structure of complex **4** consists of a discrete trinuclear complex of formula $[Ni_3L_2(O_2CPh)_4]$ (Figure 4). Selected bond lengths and angles are summarized in Table 5. The trinuclear structure possesses crystallographic C_2 symmetry with the 2-fold axis running through the central nickel atom Ni(2), resulting in a perfect linear structure. All three Ni atoms are six-coordinate with distorted octahedral environments. Each of the two terminal nickel atoms Ni(1) are coordinated by a deprotonated chelate tridentate Schiff base ligand (L) through two nitrogen atoms (N(19) and N(23)) and a phenoxo oxygen atom O(11) in a *mer* arrangement. In addition, each of the two Ni(1) ions is bonded to one of the oxygen atoms O(33) of a bridging bidentate benzoate ligand and two oxygen atoms O(41) and O(43) of a second chelating bidentate benzoate ligand. The meridionally coordinated Schiff base and the oxygen atom O(41) constitute the equatorial plane with bond distances in the range 1.998−2.141 Å (Table 6), similar to the axial ones (2.020(3) and 2.199(3) Å). The main distortion from octahedral geometry is a consequence of the small bite of the chelating benzoate ligand, the O(41)−Ni(1)−O(43) angle being only 60.8(1)°.

The coordination geometry around the central metal ion Ni(2) is also a distorted octahedron involving two bridging phenoxo oxygen atoms, O(11) and O(11′), two oxygen atoms, O(41) and O(41′) from two bridging benzoate groups and two more oxygen atoms O(31) and O(31′) from the second bridging bidentate benzoate ligand ($1\kappa O{:}2\kappa O'$). Thus one benzoate ligand bridges two nickel atoms with O(31) coordinated to Ni(2) and with O(33) to Ni(1) ($1\kappa O{:}2\kappa O'$), whereas the other benzoate ligand is bidentate to Ni(1) through the O(41) and O(43) atoms and monodentate to Ni(2) through the O(41)

(17) Bu, X.; Du, H.; Zhang, M. L.; Liao, D.-Z.; Tang, J.-K.; Zhang, R.-H.; Shionoya, M. *J. Chem. Soc., Dalton Trans.* **2001**, 593.

(18) (a) Dey, S. K.; Fallah, M. S. E.; Ribas, J.; Matsushita, T.; Gramlich, V.; Mitra, S. *Inorg. Chim. Acta* **2004**, *357*, 1517. (b) Horn, A.; Fim, L.; Bortoluzzi, A. J.; Szpoganicz, B.; de, M.; Silva, S.; Novak, M. A.; Neto, M. B.; Eberlin, L. S.; Catharino, R. R.; Eberlin, M. N.; Fernandes, C. *J. Mol. Struct.* **2006**, *797*, 154.

(19) (a) Akay, A.; Arici, C.; Atakol, O.; Fuess, H.; Svoboda, I. *J. Coord. Chem.* **2006**, *59*, 933. (b) Elmali, A.; Elerman, Y.; Svoboda, I.; Fuess, H.; Griesar, K.; Haase, W. *Z. Naturforsch., B* **1996**, *51*, 665. (c) Reglinski, J.; Morris, S.; Stevenson, D. E. *Polyhedron* **2002**, *21*, 2167. (d) Ulku, D.; Ercan, F.; Atakol, O.; Dincer, F. N. *Acta Crystallogr., Sect. C* **1997**, *53*, 1056. (e) Mukherjee, P.; Drew, M. G. B.; Gómez-Garcia, C. J.; Ghosh, A. DOI:10.1021/ic802385c.

Table 5. Bond Distances (Å) and Angles (deg) in the Metal Coordination Spheres of Complex **4**[a]

atoms	distance	atoms	distance
Ni(1)−O(33)′	2.020(3)	Ni(2)−O(11)	2.062(3)
Ni(1)−O(41)	2.141(3)	Ni(2)−O(41)	2.115(3)
Ni(1)−O(43)	2.199(3)	Ni(2)−O(31)	1.996(3)
Ni(1)−O(11)	2.045(3)	Ni(2)−O(31)′	1.996(3)
Ni(1)−N(19)	1.998(4)	Ni(2)−O(11)	2.062(3)
Ni(1)−N(23)	2.090(4)	Ni(2)−O(41)	2.115(3)
atoms	angle	atoms	angle
N(19)−Ni(1)−O(11)	88.68(14)	O(31)−Ni(2)−O(31)′	176.49(18)
N(19)−Ni(1)−O(33)′	100.26(15)	O(31)−Ni(2)−O(11)′	91.85(11)
O(11)−Ni(1)−O(33)′	91.87(12)	O(31)−Ni(2)−O(11)	90.24(11)
N(19)−Ni(1)−N(23)	95.97(15)	O(11)−Ni(2)−O(11)′	106.85(17)
O(11)−Ni(1)−N(23)	175.35(13)	O(31)−Ni(2)−O(41)′	89.86(11)
N(23)−Ni(1)−O(33)′	87.47(14)	O(41)−Ni(2)−O(11)′	170.82(12)
N(19)−Ni(1)−O(41)	156.67(14)	O(31)−Ni(2)−O(41)	87.63(12)
O(11)−Ni(1)−O(41)	82.11(11)	O(11)−Ni(2)−O(41)	82.32(11)
O(41)−Ni(1)−O(33)′	101.41(12)	O(41)−Ni(2)−O(41)′	88.51(16)
N(23)−Ni(1)−O(41)	93.50(13)		
N(19)−Ni(1)−O(43)	98.17(14)		
O(11)−Ni(1)−O(43)	91.00(12)		
O(43)−Ni(1)−O(33)′	161.40(12)		
N(23)−Ni(1)−O(43)	88.19(14)		
O(41)−Ni(1)−O(43)	60.83(11)		

[a] Symmetry code ′ = $-x$, $0.5 - y$, $1 - z$.

Table 6. Bond distances (Å) and Angles (deg) in the Metal Coordination Spheres of Complex **5**[a]

atoms	distance	atoms	distance
Ni(1)−O(11)	2.032(2)	Ni(2)−O(11)	2.078(2)
Ni(1)−O(31)	2.099(2)	Ni(2)−O(31)	2.043(2)
Ni(1)−ON(53)	2.098(2)	Ni(2)−ON(52)	2.084(2)
Ni(1)−N(19)	2.046(2)	Ni(2)−N(39)	2.034(2)
Ni(1)−N(23)	2.104(2)	Ni(2)−N(43)	2.093(2)
Ni(1)−N(61)	2.158(3)	Ni(2)−O(63)′	2.159(2)
atoms	angle	atoms	angle
O(11)−Ni(1)−N(19)	88.13(9)	N(39)−Ni(2)−O(31)	88.27(9)
O(11)−Ni(1)−ON(53)	86.47(9)	N(39)−Ni(2)−O(11)	163.91(9)
N(19)−Ni(1)−ON(53)	91.82(10)	O(31)−Ni(2)−O(11)	75.64(8)
O(11)−Ni(1)− O(31)	75.42(8)	N(39)−Ni(2)−ON(52)	92.11(10)
N(19)−Ni(1)−O(31)	163.48(9)	O(31)−Ni(2)−ON(52)	86.03(9)
ON(53)−Ni(1)−O(31)	85.70(9)	O(11)− Ni(2)−ON(52)	86.94(9)
O(11)−Ni(1)−N(23)	172.03(8)	N(39)−Ni(2)−N(43)	96.98(10)
N(19)−Ni(1)−N(23)	97.97(10)	O(31)−Ni(2)−N(43)	173.48(8)
ON(53)−Ni(1)−N(23)	88.21(10)	O(11)−Ni(2)−N(43)	99.08(9)
O(31)−Ni(1)−N(23)	98.28(8)	ON(52)−Ni(2)−N(43)	89.89(10)
O(11)−Ni(1)−N(61)	97.88(9)	N(39)−Ni(2)−O(63)′	84.89(9)
N(19)−Ni(1)−N(61)	85.73(10)	O(31)−Ni(2)−O(63)′	90.17(8)
ON(53)−Ni(1)−N(61)	174.93(10)	O(11)−Ni(2)−O(63)′	94.92(8)
O(31)−Ni(1)−N(61)	97.89(8)	ON(52)−Ni(2)−O(63)′	175.23(9)
N(23)−Ni(1)−N(61)	87.73(10)	N(43)−Ni(2)−O(63)′	94.15(9)

[a] Symmetry code ′ = $-0.5 + x$, $1.5 - y$, z.

atom ($1\kappa O$:$2\kappa^2 O,O'$). Ni(1) and Ni(2) atoms are separated by 3.019(4) Å, indicating the absence of any bond between the two nickel centers. The Ni(1)−O(11)−Ni(2) and Ni(1)−O(41)−Ni(2) bridge angles are 94.61(9) and 90.35(9)°, respectively. The six-member ring comprising the Ni(1) ion, the imine N atom, three propylene C atoms, and the amino N atom adopts a half-chair conformation, whereas that containing the aromatic moiety is distorted from planarity (maximum r.m.s. deviation 0.20 Å) toward a boat conformation. The distortion of this latter ring is greater than in **1**, **2**, or **3** presumably because of the greater steric constraints in the trinuclear complex. The amino N(23)−H does not form any hydrogen bonds.

There are several reports of trinuclear Ni(II) compounds of tetradentate Schiff base along with bridging carboxylate ions. However, tridentate Schiff base ligand has been used very rarely to synthesize such complexes. Only two examples are reported but both with the reduced Schiff base ligands, N-(2-hydroxybenzyl)propanolamine[14b] and 2-methyl-2-(2-methyl-benzylamino)-propan-1-ol,[14c] and it is proposed that the higher flexibility of the reduced Schiff base is responsible for the formation of the trinuclear complexes. Moreover, in both complexes, the nickel centers are bridged by monodentate and bidentate acetate as well as by a phenoxo group. The ($1\kappa O$:$2\kappa^2 O,O'$) bridging mode of one of the benzoate ligands found in complex **4** is rare for monocarboxylate ligands and has been only found in some dinuclear Ni(II) complexes,[20] in one trinuclear complex,[19e] and in one tetranuclear Ni(II) complex,[21] but as far as we know, this is the first example of a trinuclear Ni(II) complex with this bridging mode of a benzoate ligand.

Structure of $[Ni_2L_2(NO_2)_2]_n$ (5). The molecular structure of complex **5** contains neutral dimeric units formulated as $Ni_2L_2(NO_2)_2$ (Figure 5a), which are further joined together by nitrite bridges that link two Ni(II) ions through a Ni−O−N−Ni bridge ($1\kappa N$:$2\kappa O$) to form a one-dimensional chain running parallel to the *c* axis, as shown in Figure 5b. Selected bond lengths and angles are summarized in Table 6. The dimeric unit, $Ni_2L_2(NO_2)_2$, consists of two independent nickel atoms, Ni(1) and Ni(2), both presenting an octahedral environment formed by a deprotonated tridentate Schiff base ligand, L, a phenoxo oxygen atom from the Schiff base ligand coordinated to the other Ni(II) atom, and two nitrite ligands. The only difference in the coordination environments of the two Ni(II) ions is that Ni(1) is coordinated to a nitrogen atom, N(61), of the ordered nitrite ligand, whereas Ni(2) is coordinated to the oxygen atom, O(63) of a symmetry-related ordered nitrite ligand (Figure 5b). Both Ni(II) atoms are also linked through a disordered nitrite ligand (Figure 5a, see below). The two six-member chelate rings around Ni(1) and Ni(2) incorporating the propyl fragment from the Schiff base ligand show half-chair conformations, whereas the rings incorporating the aromatic residue are slightly distorted from planarity (maximum r.m.s. deviations 0.15, 0.17 Å) toward a screw-boat conformation. In the dimeric unit, the nitrite geometry is consistent with that found in other *cis*-μ-nitrito (*N*,*O*) nickel complexes with the bond from nitrogen to the bonding oxygen(1.298(3) Å) longer than the bond to the non-bonding oxygen (1.213(3)Å). The O−N−O bond angle (116.9(3)°) is also in the expected range. In the dimeric unit, there is disorder in the nitrite bridge between the two nickel atoms in which two possible orientations are found, as is usually observed in this kind of compounds.[7] One of the two possible orientations is shown in Figure 5a with Ni(1) bonded to O(53) and Ni(2) to N(52). In the second possible orientation the positions of these N and O atoms are

(20) (a) Adams, H.; Clunas, S.; Fenton, D. E.; Gregson, T. J.; McHugh, P. E.; Spey, S. E. *Inorg. Chim. Acta* **2003**, *346*, 239. (b) He, C.; Lippard, S. J. *J. Am. Chem. Soc.* **2000**, *122*, 184. (c) Wages, H. E.; Taft, K. L.; Lippard, S. J. *Inorg. Chem.* **1993**, *32*, 4985. (d) Sidorov, A. A.; Fomina, I. G.; Malkov, A. E.; Reshetnikov, A. V.; Aleksandrov, G. G.; Novotortsev, V. M.; Nefedov, S. E.; Eremenko, I. L. *Izv. Akad. Nauk, SSSR. Ser. Khim. (Russ.) (Russ. Chem. Bull.)* **2000**, 1915.

(21) Reglinski, J.; Taylor, M. K.; Kennedy, A. R. *Inorg. Chem. Commun.* **2006**, *9*, 736.

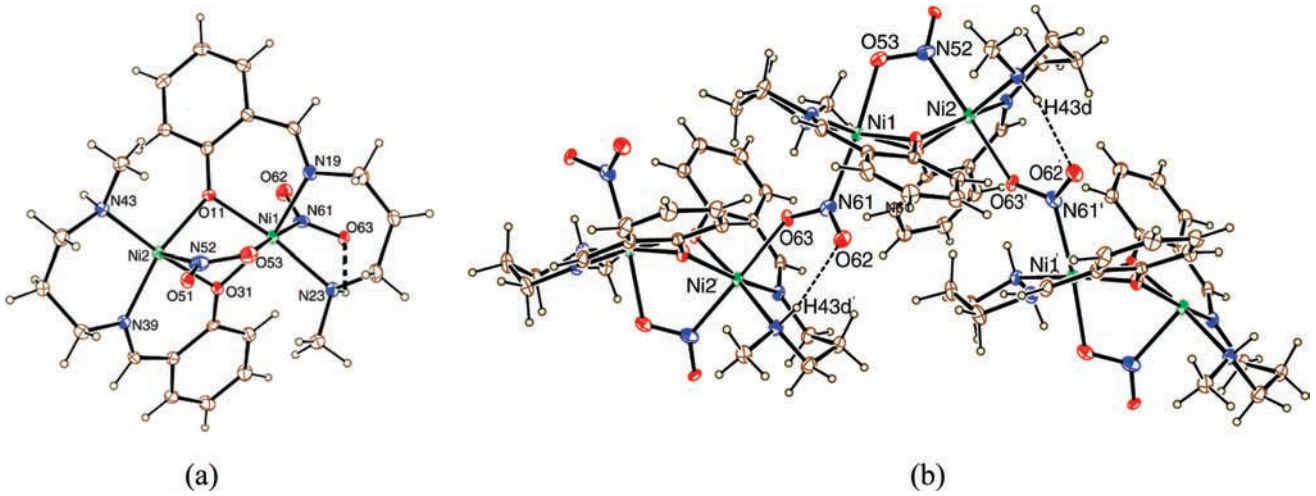

Figure 5. (a) ORTEP-3 view of the asymmetric unit of **5** with ellipsoids at the 50% probability level, (b) polymeric structure of complex **5**

reversed, and thus, the noncoordinated oxygen atom, O(51), changes its position and appears as an additional oxygen atom, O(54) (not shown in Figure 5a). Accordingly, atoms 52 and 53 were refined as 50% O and 50% N, whereas atoms O(51) and O(54) as 50% O only. In addition to this disordered nitrite bridging, there is an additional bridging nitrite that is bonded through a nitrogen atom, N(61), to Ni (1) (as shown in Figure 5a) and through an oxygen atom, O (63), to Ni(2)′ (′ = 0.5 + x, 1.5 − y, z) with a trans-N,O bridging mode (1κN:2κO) to give a one-dimensional chain as shown in Figure 5b. This bridge is strengthened by an intermolecular hydrogen bond between the H atom bonded to N(43) and the oxygen atom O(62)′ (x − 0.5, 1.5 − y, z) with dimensions H···O = 2.17 Å, N−H···O = 147°, and N···O = 2.976(3) Å (see Table S1 in the Supporting Information). There is also an intramolecular hydrogen bond between the H atom bonded to N(23) and the oxygen atom O(63) with dimensions H···O = 2.21 Å, N−H···O = 129°, and N···O = 2.870(3) Å (see Table S1 in the Supporting Information and Figure 5a).

A literature survey shows that the *trans-N,O* bridging mode of the nitrite forms infinite one-dimensional chains,[7] whereas the *cis-N,O* bridging mode, which is comparatively rare, gives rise to finite structures.[22] As far as we know, complex **5** is the first reported compound where nitrite ligands show both types of coordination modes (*cis* inside the dimer and *trans* connecting the dimers) in a single compound.

Magnetic Properties. The thermal variation of the product of the molar magnetic susceptibility times the temperature ($\chi_m T$) per two Ni(II) ions for compounds **1**−**3** is displayed in Figure 6. As can be seen, the three compounds show room temperature $\chi_m T$ values of ca. 2.3−2.4 emu K mol^{-1}, in agreement with the expected value for two noninteracting Ni(II) S = 1 ions (the expected spin only value is 2.0 emu K mol^{-1}). When lowering the temperature, compounds **2** and **3** present very similar behavior: $\chi_m T$ shows a smooth decrease at high temperatures and a more pronounced decrease as the temperature is further lowered, to reach values very close

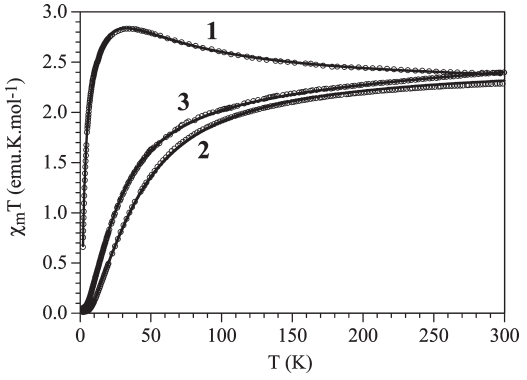

Figure 6. Thermal variation of the $\chi_m T$ product per Ni(II) dimer for compounds **1**−**3**. Solid lines show the best fit to the S = 1 dimer model (see text).

to zero at 2 K (Figure 6). Compound **1** shows a different behavior: $\chi_m T$ increases when the temperature is decreased, to reach a maximum of ca. 2.8 emu K mol^{-1} at ca. 32 K. Below this temperature, $\chi_m T$ decreases quite fast to reach a value of ca. 0.65 emu K mol^{-1} at 2 K (Figure 6).

The magnetic behavior of compound **1** indicates the presence of ferromagnetic exchange interactions within the Ni(II) dimer together with antiferromagnetic interdimer interactions and/or a zero field splitting of the resulting S = 2 spin ground state, responsible for the decrease in $\chi_m T$ at low temperatures. Because the evaluation of all the possible contributions at low temperatures in a simultaneous way results very difficult and little reliable, we have proceeded in three consecutive steps in all the cases. Thus, in a first attempt, we have fit the magnetic properties of compounds **1**−**3** to a simple S = 1 dimer model (the Hamiltonian is always written as $H = -JS_1S_2$)

$$\chi_m = \frac{N\beta^2 g^2}{kT}\frac{2e^x + 10e^{3x}}{1 + 3e^x + 5e^{3x}} \quad \text{with } x = J/kT \qquad (1)$$

In a second step, we have used the molecular field approximation expression to reproduce the interdimer antiferromagnetic coupling[23]

$$\chi^*_{dim} = \frac{\chi_{dim}}{1 - (2zJ'/Ng^2\beta^2)\chi_{dim}} \qquad (2)$$

(22) Hausmann, J.; Klingele, M. H.; Lozan, V.; Steinfeld, G.; Siebert, D.; Journaux, Y.; Girerd, J. J.; Kersting, B. *Chem. Eur.J.* **2004**, *10*, 1716 and references cited therein.

(23) O'Connor, C. J. *Prog. Inorg. Chem.* **1982**, *29*, 203.

Table 7. Magnetic Parameters and Structural Data of the Bridges on Compounds **1**−**5**

Compound	g	J (cm^{-1})	J' (cm^{-1})	c (%)	X	Ni−X (Å)[a]	Ni−X−Ni (deg)	X′	Ni−X′ (Å)[b]
1 (Ni_2)	2.116(2)	23.5(3)	−0.356(2)		N_3	2.096(3) 2.143(3)	101.61(13)		
2 (Ni_2)	2.132(2)	−24.27(6)		1.37(2)	O	2.009(2) 2.070(3)	99.75(10)		
3 (Ni_2)	2.184(3)	−16.48(4)		2.44(1)	O	2.049(3) 2.114(3)	96.60(12)	syn−*syn* −COO	2.032(3)
4 (Ni_3)	2.0283(6)	6.14(2)		4.9(1)	O	2.045(3) 2.062(3) 2.115(3) 2.141(3)	94.63(12) 90.37(11)	*syn*−*syn* −COO	1.996(3) 2.020(3)
5 (Ni_n)	2.0842(6)	−32.1(1)	−3.2(1)	0.41(6)	O	2.032(2) 2.078(2) 2.043(2) 2.099(2)	96.12(8) 95.12(8)	NO_2	2.158(3)[b] 2.160(2)[c]

[a] Ni−N bond distances in the N_3 bridges (in **1**) or Ni−O bond distances in the oxo bridges (in **2**−**5**). [b] Ni−O bond distance of the additional carboxylate (in **3** and **4**) or NO_2 bridges (in **5**). [c] Ni−N bond distance of the additional NO_2 bridge (in **5**).

where J' is the interdimer exchange interaction and χ_{dim} is the expression for an $S = 1$ dimer (eq 1). Finally, we have also used the expression derived by Ginsberg et al. for an $S = 1$ dimer with a ZFS.[24]

For compound **1**, the second model is the one that reproduces more satisfactorily the magnetic data in the whole temperature range with the following parameters (Table 7): $g = 2.116(2)$, $J = 33.9(5)$, $K = 23.5(3)$ cm^{-1} and $J' = -0.513(3)$, $K = 0.356(2)$ cm^{-1} (solid lines in Figure 6 and Figure S2 in the Supporting Information). The inclusion of a ZFS in this second model does not improve significantly the fit because the interdimer magnetic coupling and the D parameter are very closely related and their independent contributions cannot be easily accounted for.[25] This result indicates that, besides the intradimer coupling, the ZFS and the interdimer coupling are present but their correct evaluation is not possible given their close relation.

The magnetic behavior of compounds **2** and **3** indicates that both compounds present antiferromagnetic exchange interactions within the Ni(II) dimers. This antiferromagnetic interaction is also clearly seen in the thermal variation of χ_m that shows rounded maxima of ca. 0.03 and 0.04 emu mol^{-1} at ca. 35 and 25 K for compounds **2** and **3**, respectively (see Figure S2 in the Supporting Information). Accordingly, we have fitted the magnetic properties of both compounds with an antiferromagnetic $S = 1$ dimer model (eq 1) plus a paramagnetic $S = 1$ term (c) to account for the increase observed in the χ_m plot at very low temperatures in both compounds (inset in Figure S2 in the Supporting Information). This model reproduces very satisfactorily the magnetic properties of both compounds in the whole temperature range with the following parameters (Table 7): $g = 2.132(2)$, $J = -34.9(4)$, $K = -24.27(6)$ cm^{-1}, and $c = 1.37(2)$ % for compound **2** and $g = 2.184(3)$, $J = -23.71(6)$, $K = -16.48(4)$ cm^{-1}, and $c = 2.44(1)$ % for compound **3** (solid lines in Figures 6 and Figure S2 in the Supporting Information).

As in the case of compound **1**, the use of the equation of Ginsberg et al.[24] including the ZFS in compounds **2** and **3** does not improve the fit because the effect of the ZFS is observable only at low temperatures, where the presence of paramagnetic monomeric impuriries precludes a correct evaluation of this effect.[25]

The thermal variation of the $\chi_m T$ product for compound **4** per Ni(II) trimer shows a room temperature value of ca. 3.3 emu K mol^{-1}, close to the expected spin only value for three independent $S = 1$ Ni(II) ions (3.0 emu K mol^{-1}, Figure 7). When cooling the sample, $\chi_m T$ remains constant down to ca. 150 K and then shows a progressive increase to reach a maximum value of ca. 4.75 emu K mol^{-1} at ca. 5 K (inset in Figure 7). Below this temperature, χ_mT shows an abrupt decrease to reach a value of ca. 4.0 emu K mol^{-1} at 2 K. This behavior suggests that compound **4** presents a ferromagnetic coupling inside the linear centrosymmetric Ni(II) trimer as shown by the increase in $\chi_m T$ with decreasing temperatures. The sharp decease at very low temperature may be attributed to the presence of a zero field splitting in the $S = 3$ ground spin state in compound **4** and to the presence of intertrimer antiferromagnetic interactions. Thus, we have tried to fit the magnetic properties of this compound to a simple $S = 1$ linear trimer model with the Hamiltonian $H = -J(S_1S_2 + S_2S_3)$, where S_2 is the spin state of the central Ni(II) ion[26]

$$\chi_m = \frac{Ng^2\beta^2}{kT}\frac{28e^{2x} + 10e^{-x} + 2e^{-3x} + 10e^{x} + 2}{7e^{2x} + 8e^{-x} + 3e^{-3x} + 5e^{x} + e^{-2x} + 3} \quad \text{with } x = J/kT \quad (3)$$

This model reproduces very satisfactorily the magnetic behavior of compound **4** in the 5−300 K temperature range only when a paramagnetic monomeric $S = 1$ impurity was added with the following parameters (Table 7): $g = 2.0283(6)$, $J = 6.14(2)$ cm^{-1}, and $c = 4.9(1)$ % (solid line in Figure 7). We have also observed that the inclusion of an intertrimer antiferromagnetic interaction using the molecular field approximation expression (eq 2) did not reproduce the decrease at very low temperatures in a satisfactory way, confirming the existence of an additional contribution to this decrease (a ZFS in the $S = 3$ ground spin state).

The thermal variation of the $\chi_m T$ product for compound **5** per Ni(II) ion is very similar to that of compounds

(24) Ginsberg, A. P.; Martin, R. L.; Brookes, R. W.; Sherwood, R. C. *Inorg. Chem.* **1972**, *11*, 2884.
(25) Boca, R. *Coord. Chem. Rev.* **2004**, *248*, 757.
(26) (a) Rietmeijer, F. J.; Van Albada, G. A.; de Graaff, R. A. G.; Haasnoot, J. G.; Reedijk, J. *Inorg. Chem.* **1985**, *24*, 3597. (b) Carlin, R. L. *Magnetochemistry*; Springer: Berlin, 1986.

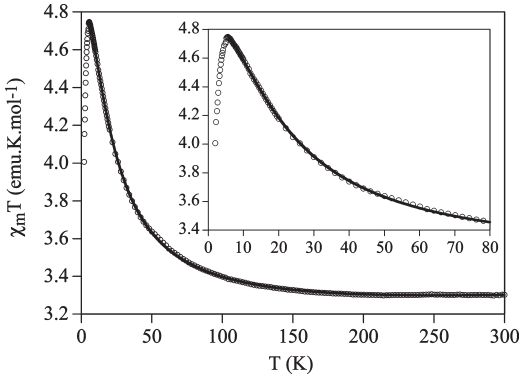

Figure 7. Thermal variation of the $\chi_m T$ product for compound **4** per Ni trimer. Inset shows the low-temperature region. Solid line shows the best fit to the model (see text).

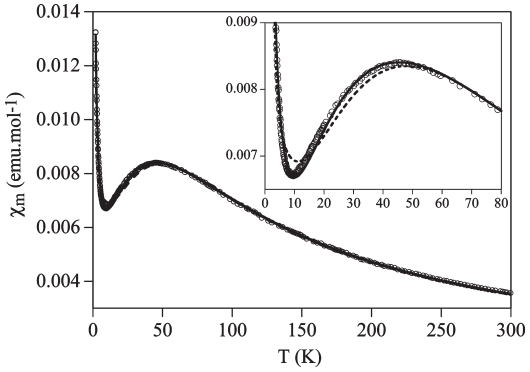

Figure 8. Thermal variation of χ_m for compound **5** per Ni(II) ion. Inset shows the low-temperature region. Solid and dashed lines are the best fit to the alternate and regular $S = 1$ chain models, respectively (see text).

2 and **3**: it shows a room temperature value of ca. 1.1 emu K mol^{-1} per Ni(II) ion (close to the expected spin only value for an $S = 1$ ion) that decreases when decreasing the temperature to reach a value close to 0 at low temperatures (not shown). This behavior suggests the presence of an overall antiferromagnetic coupling inside the chain. This antiferromagnetic coupling is confirmed by the thermal variation of the molar magnetic susceptibility per Ni(II) ion (Figure 8) that shows a rounded maximum at ca. 45 K followed by a progressive decrease and a minimum at ca. 10 K and a divergence at lower temperatures (inset in Figure 8). Because the structure of this compound shows the presence of a Ni(II) chain with two alternating different bridges (see above), we have used the $S = 1$ alternating chain model of Borrás-Almenar et al.[27] Because this model uses slightly different equations for $\alpha \leq 0.5$ and $\alpha > 0.5$ (α is the J_2/J_1 ratio), we have tried both possibilities and found that the best fit is obtained for the expression derived for $\alpha \leq 0.5$

$$\chi_m = \frac{2Ng^2\beta^2}{3J_1}\frac{[x^2 + 0.5x - (0.07096 - 0.34191\alpha)]}{[x^3 + (1.136963 + 0.748419\alpha)x^2 + (1.04853272 - 0.8077223\alpha + 1.375320\alpha^2)x + (0.4447955 + 1.162769\alpha)]} \quad (4)$$

where $x = T/|J_1|$ and $\alpha = J_2/J_1$.

This model gives a very good agreement with the experimental data in the whole temperature range when a paramagnetic $S = 1$ impurity is added to reproduce the divergence at low temperatures with the following set of parameters (Table 7): $g = 2.0842(6)$, $J_1 = -46.1(1)$, $K = -32.1(1)$ cm^{-1}, $\alpha = 0.10(2)$ (i.e., $J_2 = \alpha J_1 = -4.6(1)$, $K = -3.2(1)$ cm^{-1}), and $c = 0.41(6)$ % (solid line in Figure 8).

To confirm that the regular chain model is not adequate to reproduce the magnetic properties, we have also fitted the experimental data to the regular antiferromagnetic $S = 1$ chain model.[2] The best fit to this regular model gives similar parameters ($g = 2.13(1)$, $J = -37.4(3)$, $K = -26.0(1)$ cm^{-1}, and $c = 1.2(1)$ %), but provides a worse fit and is not able to correctly reproduce the maximum nor the minimum in the χ_m plot (dashed line in Figure 8), confirming the existence of two different alternating magnetic bridges in the Ni(II) chain. Because Borrás-Almenar et al. also developed the expressions for an alternating $S = 1$ chain including single ion anisotropy ($\beta = D/|J_1|$),[27] we have also used this more complete model including the ZFS to fit the magnetic data of compound **5**. Unfortunately, as in the previous compounds, the inclusion of this extra parameter does not improve significantly the fit, probably because of the presence of the paramagnetic contribution at low temperatures, as also observed in compounds **2** and **3**.

The antiferromagnetic exchange observed in compounds **2**, **3**, and **5** leads to a diamagnetic ground spin state in these compounds, as confirmed by the isothermal magnetization measurements at 2 K, which show values lower than 0.1 μ_B at high fields, arising from the paramagnetic impurities (Figure 9). On the contrary, the ferromagnetic coupling of compounds **1** and **4** leads to $S = 2$ and $S = 3$ ground spin sates, respectively, which are also confirmed by the isothermal magnetization measurements at 2 K (Figure 9). Since there are interdimer antiferromagnetic interactions (in compound **1**) and/or zero field splitting (in both compounds), saturation is not reached at 5 T and the magnetization values at this field are lower than the expected ones of ca. 4 and ca. 6 μ_B for compounds **1** and **4**, respectively.

The ferromagnetic exchange found in complex **1** ($J = +23.5$ cm^{-1}) lays within the range observed for Ni(II) complexes with double $\mu_{1,1}$-N_3 ($1\kappa N$:$2\kappa N$) bridges: 13 out of the 17 examples reported to date present J values between $+20.1$ and $+47.6$ cm^{-1}, with an average value of $+35.1$ cm^{-1} (the other four complexes present J values of $+78$, $+10.65$, $+3.82$, and -3.54 cm^{-1}, this last case due to a exceptionally small Ni−N−Ni angle).[28] Although there have been several attempts to correlate the magnetic exchange with different structural parameters (mainly the Ni−N−Ni bond angles and Ni−N bond distances), only a rough magnetostructural correlation with the Ni−N−Ni bond angle has been established.[28,29] Ruiz et al. have performed DFT calculations on different metal complexes with double $\mu_{1,1}$-N_3 bridges and have shown that the J value presents a weak dependence on the Ni−N−Ni bond angle.[28] Albeit, because compound **1**

(27) Borrás-Almenar, J. J.; Coronado, E.; Curely, J.; Georges, R. *Inorg. Chem.* **1995**, *34*, 2699.

(28) Ruiz, E.; Cano, J.; Alvarez, S.; Alemany, P. *J. Am. Chem. Soc.* **1998**, *120*, 11122.

(29) Ribas, J.; Escuer, A.; Monfort, M.; Vicente, R.; Cortés, R.; Lezama, L.; Rojo, T. *Coord. Chem. Rev.* **1999**, *193*, 1027.

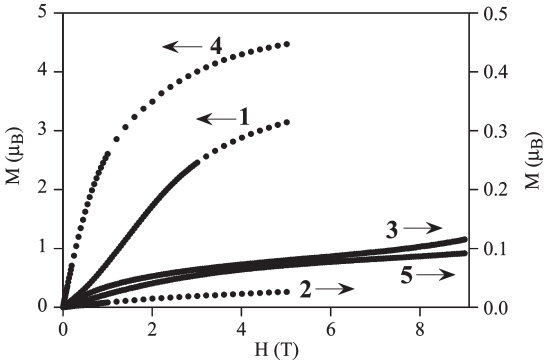

Figure 9. Isothermal magnetizations for compounds **1**−**5** at 2 K.

presents a Ni−N−Ni bond angle and Ni−N bond distances that are very similar to those found in most of the similar complexes with double $\mu_{1,1}$-N_3 bridges, the J value obtained in compound **1** is not surprising.

The magnetic coupling found in compounds **2** and **3** (J = −24.27 and −16.48 cm^{-1}, respectively) are in agreement with the magnetostructural correlations established for oxo-bridged Ni(II) complexes mainly from the Ni−O−Ni bond angles.[30] These correlations have clearly established that for Ni−O−Ni angles close to 90°, the magnetic coupling is ferromagnetic. As the Ni−O−Ni angle deviates from 90°, the ferromagnetic coupling decreases and becomes antiferromagnetic at values ca. 97−98°. The Ni−O−Ni bond angles observed in compounds **2** and **3** (99.75(10) and 96.60(12)°, respectively, Table 7 and Figure 10) indicate that compound **2** should show a moderate antiferromagnetic coupling, in agreement with the experimental results, and that compound **3** should show a weak magnetic coupling (either ferro- or antiferromagnetic, because the Ni−O−Ni bond angle is close to the crossing point between the ferro- and antiferromangetic coupling). The experimental coupling found in compound **3** (−16.48 cm^{-1}) exceeds the expected value and indicates that the additional *syn*−*syn* carboxylato bridge present in complex **3** (Figure 10) is also contributing to the overall magnetic coupling observed in this compound. Because *syn*−*syn* carboxylato bridges are well-known to promote weak or moderate antiferromagnetic coupling,[31] compound **3** is therefore expected to present an additional antiferromagnetic contribution, in agreement with the experimental results. Interestingly, there is at least one Ni(II) dimer presenting a very similar bridge to that of compound **3** (one *syn*−*syn* carboxylato bridge and two oxo bridges with Ni−O−Ni bond angles of 96.9(2) and 97.9(2)° and Ni−O bond distances of 2.024(4) and 2.028(5) Å).[18] In this very similar Ni(II) dimer, the magnetic coupling found is J = −11.98 cm^{-1}, close to the value observed in compound **3**.

The ferromagnetic coupling in compound **4** (J = 6.14 cm^{-1}) also agrees with the expected behavior from the aforementioned magneto structural correlation established for

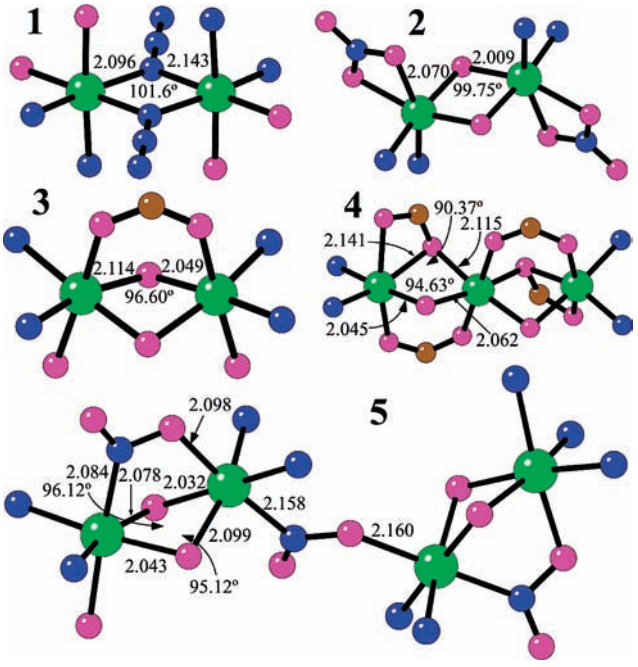

Figure 10. Structure of the Ni(II) environments in compounds **1**−**5** with the bridging bond distances (in Å) and angles (deg). Color code: N = blue, O = pink, Ni = green, C = brown.

oxo-bridged Ni(II) complexes. Thus, the two Ni−O−Ni bond angles connecting the Ni(II) ions (90.37(11) and 94.63(12)°) are within the expected range for ferromagnetic coupling, and therefore, it is not surprising to find a ferromagnetic coupling in this complex. Albeit, from the almost linear relationship between the Ni−O−Ni bond angle and the J value, the estimated coupling constant should be ca. 15−20 cm^{-1}. A possible reason explaining the lower experimental value may be, as in complex **3**, the presence of an additional *syn*−*syn* carboxylato bridge whose contribution to the overall magnetic coupling is expected to be weak or moderate antiferromagnetic.

Finally, compound **5** presents two types of bridges along the chain: a first one formed by a nitrite −NO− bridge (1κN:2κO) together with a double oxo bridge (similar to that found in complexes **2** and **3**) alternating with a second bridge formed only by a *trans*- nitrite −NO− bridge (1κN:2κO) (Figure 10). The Ni−O−Ni bond angles of the two oxo-bridges (95.12(8) and 96.12(8)°, Figure 10 and Table 7) suggest that this bridge should be weakly ferromagnetic. On the other side, the nitrite bridges with a Ni−N−O−Ni configuration (1κN:2κO) are well-known to provide moderate antiferromagnetic coupling.[7d,7f,32] Therefore, compound **5** is expected to present moderate antiferromagnetic coupling through the single nitrito bridge and a weak ferro- or antiferromagnetic coupling through the bridge formed by a nitrito and a double oxo bridge (depending on the relative values of both couplings). Because the fitting of the magnetic properties of compound **5** provides moderate antiferromagnetic coupling (−32.1 cm^{-1}) for one of the bridges and weak antiferromagnetic coupling (−3.2 cm^{-1}) for the other one, it is quite straightforward to assign the

(30) (a) Halcrow, M. A.; Sun, J. S.; Huffman, J. C.; Christou, G. *Inorg. Chem.* **1995**, *34*, 4167. (b) Clemente-Juan, J. M.; Coronado, E.; Galán-Mascarós, J. R.; Gómez-García, C. J. *Inorg. Chem.* **1999**, *38*, 55. (c) Clemente-Juan, J. M.; Chansou, B.; Donnadieu, B.; Tuchages, J. P. *Inorg. Chem.* **2000**, *39*, 5515.

(31) Fortea, A. R.; Alemany, P.; Alvarez, S.; Ruiz, E. *Chem. Eur. J.* **2001**, *7*, 627.

(32) (a) Blake, A. J.; Hill, S. J.; Hubberstey, P. *Chem. Commun.* **1998**, 1587. (b) Tolman, W. B. *Inorg. Chem.* **1991**, *30*, 4877. (c) Begley, M. J.; Hubberstey, P.; Stroud, J. *J. Chem. Soc., Dalton Trans.* **1996**, 4295.

stronger antiferromagnetic coupling (-32.1 cm^{-1}) to the single nitrito bridge and the weaker antiferromagnetic coupling (-3.2 cm^{-1}) to the bridge formed by a nitrito and a double oxo-bridge.

Conclusions

The five compounds formed by the Schiff base ligand, 2-[(3-methylamino-propylimino)-methyl]-phenol demonstrate nicely the key role played by simple monoanionic ligands as N_3^-, NO_3^-, $PhCOO^-$ and NO_2^- in determining the structure and magnetic properties of the Ni(II) complexes. The compounds constitute a unique series that show explicitly the competitive as well as the cooperative role of the monoanion and phenoxo group in bridging the metal ions. Thus, compound **1** ($[Ni_2L_2(N_3)_2(H_2O)_2]$) represents an example of a doubly bridged 1,1-N_3 Ni(II) complex with a N,N,O-Schiff base ligand, whereas compound **2** ($[Ni_2L_2(NO_3)_2]$) presents a diphenoxo-bridged complex having a rare facial coordination of the Schiff base ligand. The results clearly illustrate that bridging ability of the azide ion is greater than that of phenoxo. On the other hand, the benzoate ion in complexes **3** and **4** and nitrite ion in **5** do not compete with the phenoxo group to bridge the metal ions, instead act as additional bridges to facilitate the formation of the variety of interesting polynuclear complexes. As is observed, the benzoate ion yielded a rare example of a triply bridged Ni(II) dimer ($[Ni_2L_2(O_2CPh)(CH_3OH)_2]ClO_4 \cdot 0.5CH_3OH$ (**3**) (with two oxo and one *syn*−*syn* carboxylate bridges) and the first example of a Ni(II) trimer $[Ni_3L_2(O_2CPh)_4]$ (**4**) with a benzoate ligand presenting a $1\kappa^2OO':2\kappa O$ coordinating mode, whereas the nitrite ligands produce compound **5** ($[Ni_2L_2(NO_2)_2]_n$) which is the first example of a complex containing nitrite ligands with both cis and trans $1\kappa N:2\kappa O$ coordinating modes in the same compound. From the magnetic point of view, this series of complexes show that the differences observed in the structures of the Ni(II) complexes also imply important changes in the magnetic properties. Thus, complexes **2** and **3** are antiferromagnetically coupled dimers whereas complex **1** is a ferromagnetically coupled dimer. Complex **4** is a rare example of ferromagnetically coupled Ni(II) trimer and compound **5** is an alternating antiferromagnetic S = 1 chain. The magnetic properties of all five compounds have been reproduced very satisfactorily in the whole temperature range with the corresponding magnetic models. This series of complexes is thus a revelation of the importance of anions in constructing polynuclear complexes with versatile structures and tunable magnetic properties. They open up a new possibility for the synthesis of desired materials by changing merely the anion that is very rarely taken into consideration. The use of many other similar Schiff base ligands combined with other simple monoanionic ligands is expected to lead to novel series of compounds with different and original structures and magnetic properties. This work is underway.

Acknowledgment. We thank CSIR, Government of India [Junior Research Fellowship to P.M, Sanction no. 09/028 (0663)/2006-EMR-I], the European Union (MAGMANet network of excellence) and the Spanish Ministerio de Educación y Ciencia (Projects MAT2007-61584 and Consolider-Ingenio 2010 CSD 2007-00010 in Molecular Nanoscience). We also thank EPSRC and the University of Reading for funds for the X-Calibur system.

Supporting Information Available: Crystallographic information files; additional figures and table (PDF). This material is available free of charge via the Internet at http://pubs.acs.org.